2012 IEEE/RSJ International Conference on
Intelligent Robots and Systems
October 7-12, 2012. Vilamoura, Algarve, Portugal

Iterative Learning Control for a Musculoskeletal Arm: Utilizing Multiple Space Variables to Improve the Robustness

Kenji Tahara, Yuta Kuboyama and Ryo Kurazume

***Abstract*— In this paper, a new iterative learning control method which uses multiple space variables for a musculoskeletal-like arm system is proposed to improve the robustness against noises being included in sensory information. In our previous works, the iterative learning control method for the redundant musculoskeletal arm to acquire a desired end-point trajectory simultaneous with an adequate internal force was proposed. The controller was designed using only muscle space variables, such as a muscle length and contractile velocity. It is known that the movement of the musculoskeletal system can be expressed in a hierarchical three-layered space which is composed of the muscle space, the joint space and the task space. Thus, the new iterative learning control input is composed of multiple space variables to improve its performance and robustness. Numerical simulations are conducted and their result is evaluated from the viewpoint of the robustness to noises of sensory information. An experiment is performed using a prototype of musculoskeletal-like manipulator, and the practical usefulness of the proposed method is demonstrated through the result.**

I. INTRODUCTION

There is no doubt that human's natural movements are still more smooth, dexterous and sophisticated than present robotic systems. Recently, the realization of robots that behave smoothly and softly as with humans is highly expected in order to help us in our daily life. Particularly, modeling of a control strategy of human body movements is quite valuable for robots operated around our living space in this regard. It is well-known in physiological and kinesiological fields that the human's natural movements are performed by an adequate combination of a sensory feedback manner using several external sensors such as a vision or tactile sensor and a feed-forward manner obtained through sophisticated learning and estimation strategies [1], [2]. Thus, not only how to design both the feedback and feed-forward control strategies, but also how to merge them adequately is important to acquire the human's natural movements.

Meanwhile, it is well-known in robotics field that an iterative learning control method is quite effective for robots to acquire a desired time-dependent movement [3], [4]. This method is composed of a feedback manner and a feed-forward manner similar to the human's control strategy. Before learning, the control input is composed only of the feedback manner, and then the control signal gradually governed by the feed-forward manner according to the increase of the number of trials. Eventually, the control input is mostly composed of the feed-forward control manner after learning well through several trials. The method is quite robust to modeling errors and unknown parameters.

Until now, we have utilized the iterative learning control scheme to a musculoskeletal arm model whose muscle model owns a strong nonlinear characteristics [5], [6]. A desired time-dependent end-point trajectory with an adequate internal force can be obtained by using the proposed method. In the previous works, the desired time-dependent trajectory was designed in the task space, and the control signal was designed in the muscle length space by computing inverse kinematics from the task space to the muscle space. Thus, the controller consisted only of the muscle space variables, such as a length and contractile velocity of the muscle. Meanwhile, the movement of the musculoskeletal system can be expressed not only in the muscle space, but also the joint space, or the task space. These spaces make a three-layered structure, and the dynamics of the system and its controller can also be expressed in each space. The performance of the controller partially depends on which space the controller is designed in, and thereby it is important and valuable to discuss which space is better to design the controller. Additionally, it is inevitable that sensory information includes noises. For instance, it is known that the muscle information, which can be measured as EEG, includes a lot of noises. Since the kind of included noises is different in each space, their effect to the movement is also different. There is a possibility to be able to improve the learning controller to be robust to these noises by using plural space variables in this regard.

In this study, a new iterative learning control method is proposed which utilizes plural space variables to improve its performance and robustness against noises. The iterative learning control input is basically composed of a linear summation of a sensory feedback part and a feed-forward part obtained through the iterative learning process. The proposed control input utilizes different space variables to compose the feedback part and the feed-forward part to be robust to these noises. In what follows, firstly a two-link six-muscle musculoskeletal planar arm is modeled in Section II. Secondly, a nonlinear muscle model based on a physiological study is presented in Section III. Next, the validity of the proposed controller is shown by numerical simulation results in Section IV. Finally, the practical usefulness of the proposed controller is demonstrated through an experimental

K. Tahara is with Faculty of Engineering, Kyushu University, 744 Moto'oka, Nishi-ku, Fukuoka 819-0395, Japan. tahara@ieee.org
Y. Kuboyama is with Graduate School of Information Science and Electrical Engineering, Kyushu University, 744 Moto'oka, Nishi-ku, Fukuoka 819-0395, Japan. kuboyama@irvs.ait.kyushu-u.ac.jp
R. Kurazume is with Faculty of Information Science and Electrical Engineering, Kyushu university, 744 Moto'oka, Nishi-ku, Fukuoka 819-0395, Japan. kurazume@ait.kyushu-u.ac.jp

978-1-4673-1735-1/12/S31.00 ©2012 IEEE

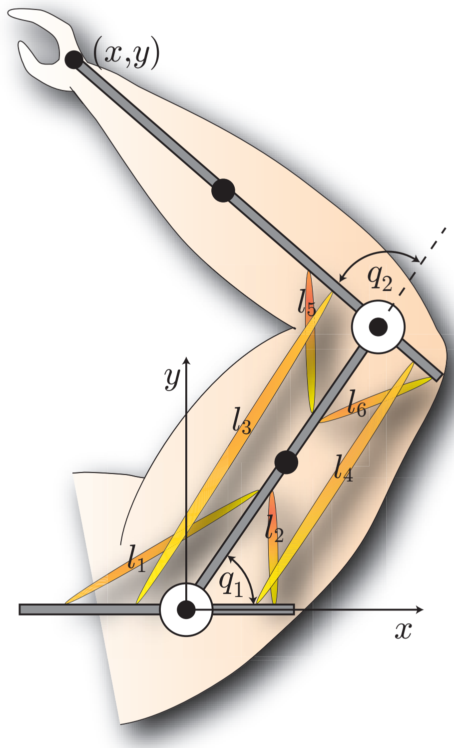

Fig. 1. Two-link six-muscle musculoskeletal arm model

result in Section V.

II. Two-Link Six-Muscle Musculoskeletal Arm Model

Figure 1 shows a musculoskeletal arm model used in this study. The model is composed of two rigid links and four mono-articular muscles and two bi-articular muscles. This is a planar arm and then its movement is limited within a horizontal plane. Therefore the gravity effect is ignored. Each muscle is approximated as a linear segment, and assuming that the mass of the muscles is included into the mass of each link. Note that the mesurable variables are the position of the end-point and its velocity a visual sensor, and each muscle length and its contractile velocity by an encoder instead of a muscle spindle.

A. Kinematics

The forward kinematics from the joint angle to the muscle length is given as follows:

$$\boldsymbol{l} = \boldsymbol{G}_l(\boldsymbol{q}) \in \mathbb{R}^6, \tag{1}$$

where $\boldsymbol{l} = [l_1, l_2, \cdots, l_6]^{\mathrm{T}} \in \mathbb{R}^6$ denotes the vector of the muscle length, $\boldsymbol{q} = [q_1, q_2]^{\mathrm{T}} \in \mathbb{R}^2$ denotes the vector of the joint angle. Also, $\boldsymbol{G}_l(\boldsymbol{q})$ in (1) is a nonlinear vector function that expresses the relation between each joint angle and each muscle length. The time derivertive of (1) is given as follows:

$$\dot{\boldsymbol{l}} = \boldsymbol{W}^{\mathrm{T}}\dot{\boldsymbol{q}} \in \mathbb{R}^6, \tag{2}$$

where $\boldsymbol{W}^{\mathrm{T}} \in \mathbb{R}^{6\times2}$ is the Jacobian matrix for each muscle contractile velocity with respect to each joint angular velocity, and it is called "the muscle Jacobian matrix" hereinafter.

The relation between the vector of the muscular force $\boldsymbol{f}_m = [f_{m1}, f_{m2}, \cdots, f_{m6}]^{\mathrm{T}} \in \mathbb{R}^6$ which depends on a control signal to be designed in the next section, and the vector of the joint torque $\boldsymbol{\tau} = [\tau_1, \tau_2]^{\mathrm{T}} \in \mathbb{R}^2$ is given by the principle of virtual work in the following manner:

$$\boldsymbol{\tau} = \boldsymbol{W}\boldsymbol{f}_m \in \mathbb{R}^2, \tag{3}$$

Assume that $\boldsymbol{W} \in \mathbb{R}^{2\times6}$ is of row full-rank during movement, and then the inverse relation of (3) is given as follows:

$$\boldsymbol{f}_m = \boldsymbol{W}^{+}\boldsymbol{\tau} + \left(\boldsymbol{I}_6 - \boldsymbol{W}^{+}\boldsymbol{W}\right)\boldsymbol{k} \in \mathbb{R}^6, \tag{4}$$

where $\boldsymbol{W}^{+} = \boldsymbol{W}^{\mathrm{T}}(\boldsymbol{W}\boldsymbol{W}^{\mathrm{T}})^{-1} \in \mathbb{R}^{6\times2}$, $\boldsymbol{I}_6 \in \mathbb{R}^{6\times6}$ denotes an unit matrix, and $\boldsymbol{k} \in \mathbb{R}^6$ denotes an arbitrary vector. The physical meaning of the second term of the right-hand side of (4) is an internal force space which is generated by redundant muscles. In addition, the statics between $\boldsymbol{\tau}$ and the vector of the output force of the end-point in the task space $\boldsymbol{F} \in \mathbb{R}^2$ is given as follows:

$$\boldsymbol{\tau} = \boldsymbol{J}^{\mathrm{T}}\boldsymbol{F} \in \mathbb{R}^2. \tag{5}$$

where $\boldsymbol{J} \in \mathbb{R}^{2\times2}$ denotes the Jacobian matrix for the end-point velocity with respect to each joint angular velocity. Substituting (5) into (4) yields:

$$\boldsymbol{f}_m = \boldsymbol{W}^{+}\boldsymbol{J}^{\mathrm{T}}\boldsymbol{F} + \left(\boldsymbol{I}_6 - \boldsymbol{W}^{+}\boldsymbol{W}\right)\boldsymbol{k} \in \mathbb{R}^6. \tag{6}$$

Equation (6) shows the inverse relation of the statics between $\boldsymbol{f}_m$ and $\boldsymbol{F}$. Meanwhile, the forward kinematics from the joint angle $\boldsymbol{q} \in \mathbb{R}^2$ to the end-point position in the task space $\boldsymbol{x} \in \mathbb{R}^2$ is given as follows:

$$\boldsymbol{x} = \boldsymbol{G}_x(\boldsymbol{q}) \in \mathbb{R}^2, \tag{7}$$

where $\boldsymbol{G}_x(\boldsymbol{q})$ is a nonlinear vector function that expresses the forward kinematics from the joint angle to the end-point position. The time derivertive of (7) is given as follows:

$$\dot{\boldsymbol{x}} = \boldsymbol{J}\dot{\boldsymbol{q}} \in \mathbb{R}^2. \tag{8}$$

Assume that $\boldsymbol{J}$ is of full-rank, thus the inverse relation of (7) and (8) can be given in the following way:

$$\boldsymbol{q} = \boldsymbol{G}_x^{-1}(\boldsymbol{x}) \in \mathbb{R}^2 \tag{9}$$

$$\dot{\boldsymbol{q}} = \boldsymbol{J}^{-1}\dot{\boldsymbol{x}} \in \mathbb{R}^2, \tag{10}$$

where $\boldsymbol{G}_x^{-1}(\boldsymbol{x})$ denotes a nonlinear vector function which means the inverse kinematics from the end-point position to the joint angle. Also, (10) denotes the differential inverse kinematics from the end-point velocity to the joint angular velocity. Substituting (9) into (1), and (10) into (2), respectively, yields

$$\boldsymbol{l} = \boldsymbol{G}_l\left(\boldsymbol{G}_x^{-1}(\boldsymbol{x})\right) \in \mathbb{R}^6 \tag{11}$$

$$\dot{\boldsymbol{l}} = \boldsymbol{W}^{\mathrm{T}}\boldsymbol{J}^{-1}\dot{\boldsymbol{x}} \in \mathbb{R}^6. \tag{12}$$

Equations (11) and (12) show the inverse kinematics from the task space to the muscle space, and these are utilized in the feed-forward manner.

B. Nonlinear Muscle Model

A modified Hill's muscle model has been utilized in our previous works [5], [6]. It can express a nonlinearity of the skeletal muscle with respect to the muscle contractile velocity. However, it does not consider any nonlinear elasticity in which the skeletal muscle intrinsically owns. In this study, another nonlinear muscle model is newly modeled based on the Audu's model [7]. The Audu's model consists of two independent parts, an active contractile element depending on the muscle activation level, and a passive nonlinear elastic element. Since Audu's model considers only a static situation and there is no effect of the muscle contractile velocity, both active and passive viscous elements are newly added to the Audu's model in this study. The active viscous element depends on the muscle activation level, and the passive viscous element is a constant. Basically, both the viscous elements have been modeled as a part of our previously proposed model. Namely, the new muscle model includes Audu's model and a part of our previous model. It is is given as follows:

$$f_m(u,l,\dot{l}) = u - p_1 e^{p_2(l-l_0)} - (c_1 u + c_2)\dot{l}, \tag{13}$$

where $f_m(u,l,\dot{l})$ is the muscle output force, u signifies the control input to the muscle, l stands for the length of the muscle, l_0 indicates the intrinsic rest length of the muscle, $\dot{l}$ denotes the contractoin velocity of the muscle, p_1, p_2, c_1 and c_2 are a positive constant, respectively. Namely, the first term of the RHS indicates the active contractile element, the second term of the RHS indicates a passive nonlinear elastic element, and the last term of the RHS indicates both the active and passive viscous elements which are newly added to Audu's model.

III. ITERATIVE LEARNING CONTROL LAW

The PI-type iterative learning control method [8] is introduced to accomplish a given desired time-dependent trajectory. Time series error datasets regarding position and velocity are stored during one trial to compose an input for the next trial. The datasets are multiplied by the learning gains, and added to the control input for the next trial.

As mentioned in Section I, there are three candidates of state space to compose the iterative learning control input, which are the muscle space, the joint space, and the task space. Therefore, which spaces are better to compose the control input is quite important to obtain a desirable performance. In addition, it is inevitable that some noises are included into sensory information, and they strongly affect the movement of musculoskeletal system. Several different types of noises are included into the sensory information obtained from each space. Therefore, the robustness to the noises are also different according to which spaces the controller is designed in. In order to improve the robustness to the noises included into the sensory information, a new iterative learning control method is proposed which utilizes plural state space variables. In this paper, the task space is chosen to design the feedback manner, and the muscle space is chosen to design the feed-forward manner as one of the case studies. The control input to the muscles at the i^{th} trial is given as follows:

$$\begin{aligned} \boldsymbol{u}_i = &- \boldsymbol{W}_i^{+} \boldsymbol{J}_i^{\mathrm{T}} \left(\boldsymbol{K}_p \boldsymbol{\Delta x}_i - \boldsymbol{K}_v \boldsymbol{\Delta \dot{x}}_i \right) \\ &+ \left(\boldsymbol{I}_6 - \boldsymbol{W}_i^{+} \boldsymbol{W}_i \right) + \boldsymbol{v}_i, \end{aligned} \tag{14}$$

where the subscript i indicates the trial number, $\boldsymbol{K}_p = \mathrm{diag}[k_{p_1}, k_{p_2}] \in \mathbb{R}^{2\times 2} > \boldsymbol{0}$ denotes the task space position feedback gain, $\boldsymbol{K}_v = \mathrm{diag}[k_{v_1}, k_{v_2}] \in \mathbb{R}^{2\times 2} > \boldsymbol{0}$ signifies the task space velocity feedback gain, and $\boldsymbol{v}_i$ is the feed-forward term obtained through the iterative learning process. The position and velocity errors in the task space are given as $\boldsymbol{\Delta x}_i = \boldsymbol{x}_i - \boldsymbol{x}_d \in \mathbb{R}^2$ and $\boldsymbol{\Delta \dot{x}}_i = \dot{\boldsymbol{x}}_i - \dot{\boldsymbol{x}}_d \in \mathbb{R}^2$ where $\boldsymbol{x}_d$ and $\dot{\boldsymbol{x}}_d$ are the desired time-dependent end-point position and velocity trajectories in the task space, respectively. The feed-forward term $\boldsymbol{v}_i \in \mathbb{R}^6$ is designed not in the task space similar to the feedback manner, but in the muscle space, and it is updated in the following manner:

$$\boldsymbol{v}_i = \begin{cases} \boldsymbol{0} & \text{if } \ i = 1 \\ (1-\beta)\,\boldsymbol{v}_{i-1} - \left(\boldsymbol{\Phi \Delta l}_{i-1} + \boldsymbol{\Psi \Delta \dot{l}}_{i-1} \right) & \text{if } \ i > 1 \end{cases}, \tag{15}$$

where $\boldsymbol{\Phi} = \mathrm{diag}[\phi_1, \phi_1, \cdots, \phi_6] \in \mathbb{R}^{6\times 6} > \boldsymbol{0}$ and $\boldsymbol{\Psi} = \mathrm{diag}[\psi_1, \psi_2, \cdots, \psi_6] \in \mathbb{R}^{6\times 6} > \boldsymbol{0}$ are the position and velocity learning gain matrices, respectively. The position and velocity errors in the muscle space are given as $\boldsymbol{\Delta l}_i = \boldsymbol{l}_i - \boldsymbol{l}_d \in \mathbb{R}^2$ and $\boldsymbol{\Delta \dot{l}} = \dot{\boldsymbol{l}}_i - \dot{\boldsymbol{l}}_d \in \mathbb{R}^2$ where $\boldsymbol{l}_d \in \mathbb{R}^6$ and $\dot{\boldsymbol{l}}_d \in \mathbb{R}^6$ are the desired muscle length and contractile velocity associated with the given desired time-dependent end-point position and velocity trajectories in the task space $\boldsymbol{x}_d$ and $\dot{\boldsymbol{x}}_d$. They are given by computing the inverse kinematics in the following way:

$$\boldsymbol{\Delta l}_i = \boldsymbol{G}_l \left(\boldsymbol{G}_x^{-1}(\boldsymbol{x}_i) \right) - \boldsymbol{G}_l \left(\boldsymbol{G}_x^{-1}(\boldsymbol{x}_d) \right), \tag{16}$$

$$\boldsymbol{\Delta \dot{l}}_i = \boldsymbol{W}_i^{\mathrm{T}} \boldsymbol{J}_i^{-1} \boldsymbol{\Delta \dot{x}}_i. \tag{17}$$

The noises included into the sensory information are assumed to be Gaussian noise in this study. It is known that an error of the initial condition between each iterative trial, and a fluctuation of the dynamics regarding some noises make the overall system unstable when utilizing the iterative learning control method. In order to overcome the effect of the noises, Arimoto [9] has introduced a forgetting factor in the iterative update law. Using the forgetting factor guarantees that the final convergence trajectory of the system after learning well is on the vicinity of the desired trajectory. In (15), β denotes the forgetting factor, and it must be chosen so as to satisfy $0 < \beta < 1$. Assume that the sensory information of the muscle length and the end-point position, and their each velocity independently includes Gaussian noise, respectively. The magnitude of the noise for the end-point position and velocity in the task space is assumed to be up to 4% of the actual information, and that for the muscle length and contractile velocity is assumed to be up to 50% of the actual information. This is because we assume that the end-point position and velocity are measured by eyes whose obtaind

TABLE I

PHYSICAL PARAMETERS OF THE TWO-LINK SIX-MUSCLE ARM MODEL

	Length [m]	Mass [kg]	Inertial moment [kg·m^2]	CoM position [m]
1st Link	0.31	1.93	0.0141	0.165
2nd Link	0.34	1.52	0.188	0.17

TABLE II

MUSCLE PARAMETERS

Muscle	l_0 [m]	p_1	p_2	c_1	c_2
f_1	0.1	4.0	15.0	10.0	100.0
f_2	0.055	4.0	15.0	10.0	100.0
f_3	0.34	4.0	15.0	10.0	100.0
f_4	0.25	4.0	15.0	10.0	100.0
f_5	0.2	4.0	15.0	10.0	100.0
f_6	0.17	4.0	15.0	10.0	100.0

information is relatively accurate, and the muscle length and contractile velocity are measured by a muscle spindle whose obtained information includes a large electrical noise.

IV. NUMERICAL SIMULATIONS

Numerical simulation results are shown here to verify the robustness of the proposed controller. Each physical parameter and gain is shown in Table I to III. The desired time-dependent trajectory is designed subject to the minimum jerk criterion proposed by Flash and Hogan [10], which minimizes the following performance index C.

$$C = \int_0^T \|\dddot{\boldsymbol{x}}(t)\|^2 \mathrm{d}t, \tag{18}$$

where T is a duration time of the movement, and $\dddot{\boldsymbol{x}}$ stands for a jerk of the end-point in the task space. Note that the minimum jerk criterion is used in the simulation as one of the case studies, and any other physiological hypotheses can be utilized instead of the minimum jerk criterion. The desired trajectory is designed as a circle in the task space. By calculating (18), it is given as follows:

$$\boldsymbol{x}_d(t) = \boldsymbol{x}_0 + \begin{bmatrix} R\cos\left(2\pi\omega\left(\frac{t}{T}\right)\right) - R \\ R\sin\left(2\pi\omega\left(\frac{t}{T}\right)\right) \end{bmatrix} \in \mathbb{R}^2 \tag{19}$$

$$\omega\left(\tfrac{t}{T}\right) = 6\left(\tfrac{t}{T}\right)^5 - 15\left(\tfrac{t}{T}\right)^4 + 10\left(\tfrac{t}{T}\right)^3, \tag{20}$$

where $\boldsymbol{x}_0$ denotes the initial position and is set to be $[-0.02, 0.46]^{\mathrm{T}}$, and R denotes the radius of the circle and is set to be 0.1 [m]. The duration time T is set to be 1 [s].

In order to show the advantage of the new controller, three types of numerical simulations are conducted. One is using the proposed controller that is composed of both the task and muscle space variables. The others are using a conventional iterative learning controller that is composed of either the task space or the muscle space variables. As mentioned in Section III, in all the simulations, each end-point position and velocity information includes Gaussian noise whose magnitude is up to 4% of the actual information, and each muscle length and contractile velocity information includes Gaussian noise whose magnitude is up to 50% of the actual information.

TABLE III

GAINS

Feedback Gain	$\boldsymbol{K}_{tp} = 30\boldsymbol{I}_2$	$\boldsymbol{K}_{tv} = 20\boldsymbol{I}_2$
Learning Gain	$\boldsymbol{\Phi}_m = 160\mathbf{I}_6$	$\boldsymbol{\Psi} = 200\boldsymbol{I}_6$

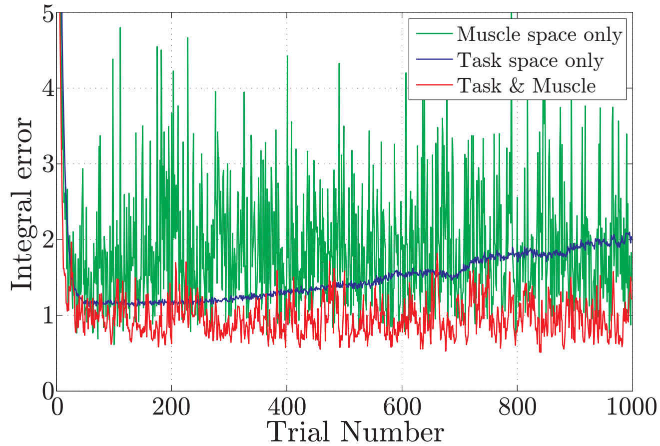

Fig. 5. History of integral square errors of the end-point position according to the number of trials: using both the task and muscle space variables, using only the task space variables, and using only the muscle space variables

Figure 2 shows the loci of the end-point position in the case of using the new controller. Figures 3 and 4 show the loci of the end-point position when the controller is designed using either the task space or the muscle space variables, respectively. We see from these figures that the end-point position trajectory in all cases mostly converges to the vicinity of the desired one according to the increase of the number of trials. Clearly, the performance of the newly proposed controller is better than that of other conventional iterative learning control methods.

Figure 5 shows the history of integral square errors of the end-point position according to the number of trials in each simulation. We see from the figure that the integral square error gradually diverges according to the increase of the number of trials when using only the task space variables. Meanwhile, the error increases and decreases intensely and its amplitude is relatively large when using only the muscle space variables, although it does not diverge unlike that of using only the task space variables. In contrast, clearly the integral square error is smaller than that of other cases in the case of using the new controller. Thus, it is confirmed that the performance of the new iterative learning controller is better than other conventional iterative learning controller, even though the sensory information includes Gaussian noises, particularly, the sensory information of the muscle space variables includes up to 50% of the actual information.

V. EXPERIMENT

An experimental result is shown here to demonstrate the practical usefulness of the proposed controller. A two-link six-muscle wire-driven planar arm developed in the study is shown in Fig. 6 Six wires, which are made of Kevlar produced by DuPont, are utilized to mimic the muscle-like

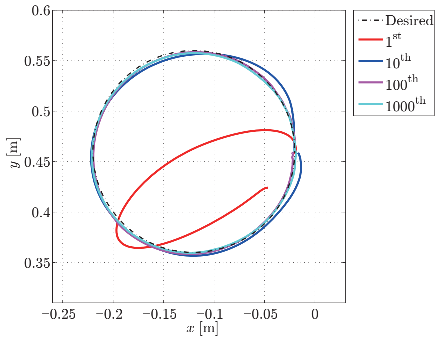

Fig. 2. Loci of the end-point position when the controller is designed using both the muscle and task space variables

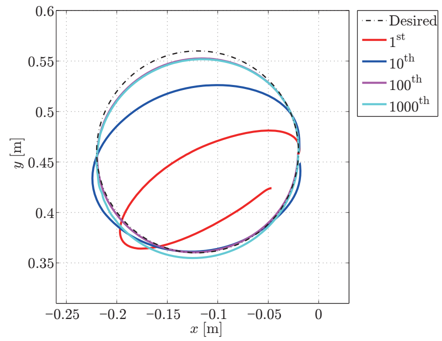

Fig. 3. Loci of the end-point position when the controller is designed using only the task space variables

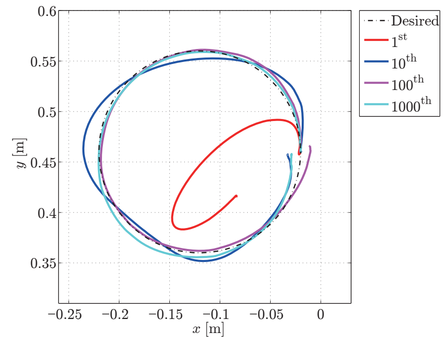

Fig. 4. Loci of the end-point position when the controller is designed using only the task space variables

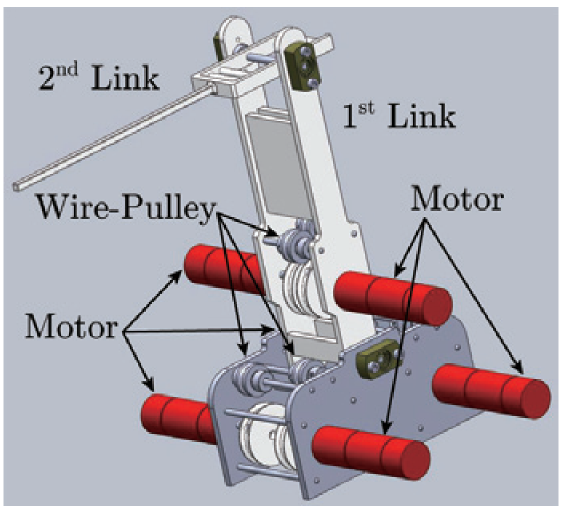

Fig. 6. Experimental setup of the two-link six-muscle wire-driven planar arm system

TABLE IV

PHYSICAL PRAMETERS OF THE EXPERIMENTAL SETUP

	Length [m]	Mass [kg]	Inertial moment [kg·m^2]	CoM position [m]
1st Link	0.21	0.97	0.063	0.05
2nd Link	0.23	0.03	0.001	0.08

driven mechanism. They are connected to each link and six DC-motors through several pulleys. Each physical parameter of the system is shown in Table IV. The actuators are produced by FAULHABER which each has a 1:13 ratio gear head and a rotary encoder. The CCD camera to measure the position of the end-point in the task space is Dragonfly2 which can capture a visual image in every 33 [ms]. The overhead view of the experimental setup is shown in Fig. 7.

In order to show the performance of the new controller for various kinds of desired trajectories, the desired end-point trajectory in the experiment is designed as a linear segment that is different from the simulation. It is given as follows:

$$\boldsymbol{x}_d(t) = \boldsymbol{x}_0 + (\boldsymbol{x}_f - \boldsymbol{x})\,\boldsymbol{\omega}\left(\tfrac{t}{T}\right) \tag{21}$$

where $\boldsymbol{x}_0 \in \mathbb{R}^2$ is the initial position, $\boldsymbol{x}_f \in \mathbb{R}^2$ is the final position of the end-point respectively, and $\boldsymbol{\omega}$ has already shown in (20). The concrete value of each $\boldsymbol{x}_0$, $\boldsymbol{x}_f$ and

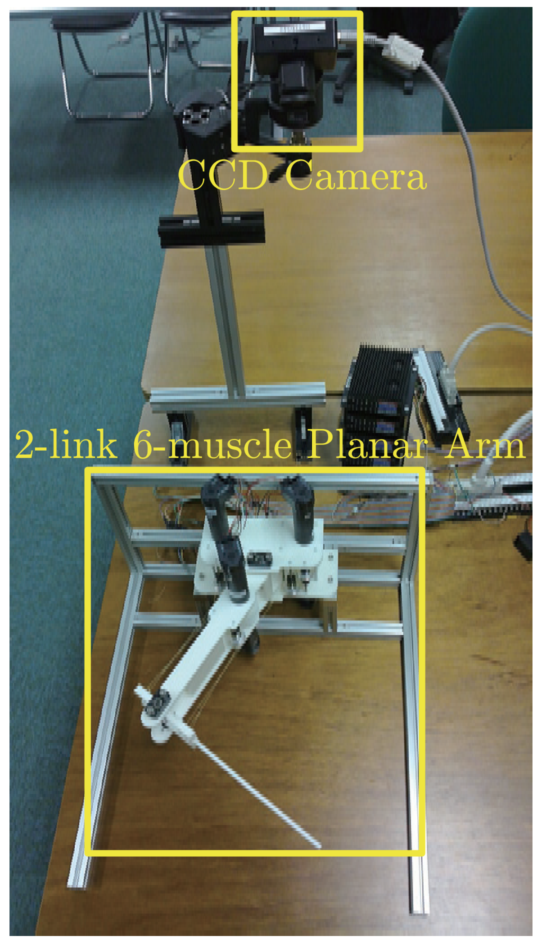

Fig. 7. Overhead view of the experimental setup

the loci of the desired trajectory are shown in Fig. 8 The duration time T is set to be 3 [s]. In the experiment, the nonlinear muscle model is computationally implemented as a soft-ware. In order to save substantial time, a numerical simulation of the iterative learning in a thousand times trials is performed, and finally acquired control input by the simulation is utilized as the initial control input for the experiment before performing the experiment. The iterative trial number is ten times in the experiment.

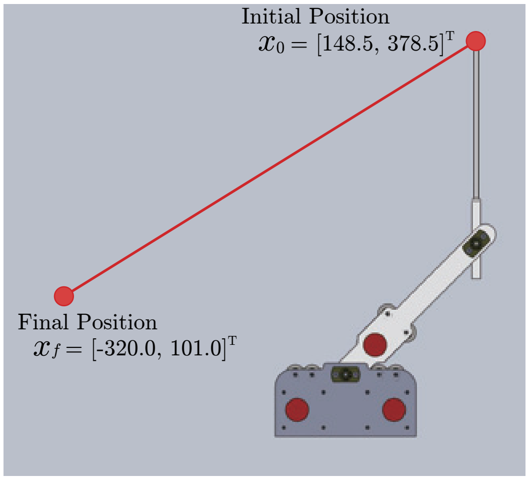

Fig. 8. Desired trajectory of the end-point in the task space

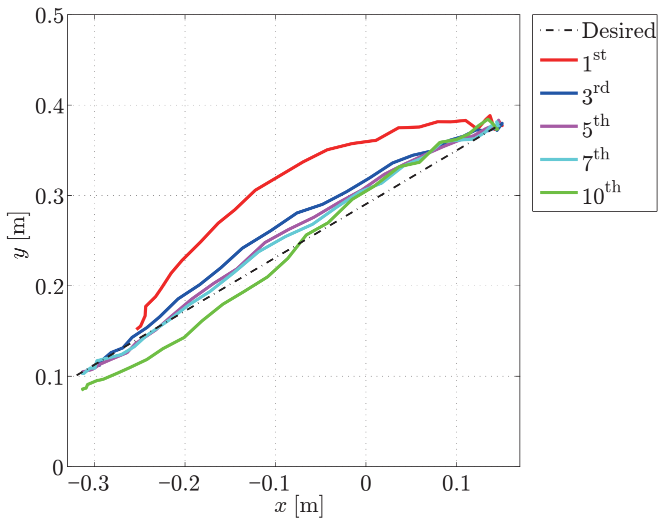

Fig. 9. Loci of the end-point position in the experiment

The loci of the end-point trajectory are shown in Fig. 9. We see from the figure that the end-point trajectory at the first trial is slightly different from the desired one, even though each gain is well-tuned. This is because there still remain certain modeling errors even though the initial control input is obtained by the deliberate simulation beforehand. The trajectory tracking error is gradually reduced according to the increase of the number of trials. In the 10^{th} trial, the trajectory of the end-point converges to the vicinity of the desired one. The remained small tracking error comes from the noise included in the visual information. Additionally, the resultant trajectories includes a little oscillation. This comes from that the experimental visual servoing system has a considerable time-delay which comes from the low sampling rate (33 [ms]) of the visual sensor. It is not serious unless high frequency-domain movements are necessary for the robot, and the error is acceptably small enough in this study. In other words, the experimental results demonstrated that the proposed iterative learning control method is practically useful even though there exist the nonlinear muscle dynamics, the noises and such time-delay.

VI. Conclusion

In this paper, the new iterative learning control method for the musculoskeletal arm system was proposed. Firstly, kinematics of the system and the nonlinear muscle dynamics were given. Next, the new iterative learning controller was designed. The controller is composed of two parts. One is the feedback input which consists of the task space variables, and the other is the feed-forward input obtained through the iterative learning process which consists of the muscle space variables. The results of numerical simulation showed that the proposed controller is more robust against the sensory noises than any conventional iterative learning control method, even though there exists the nonlinear muscle dynamics. Finally, the practical usefulness of the proposed controller was demonstrated through the experimental result. In this paper, the relation and analogy between the proposed control strategy and several physiological hypotheses were not discussed explicitly. We know that it is important to reveal such relation and analogy in order to emphasize the physiological plausibility of the proposed method. Since many physiological works dealing with the relation between the sensory feedback and feed-forward manner have been studied [11–13], we would like to develop the relation between our proposed methodology and such physiological studies in the future works. Also we would like to give the stability and convergence of the proposed controller theoretically.

References

[1] A. Polit A and E. Bizzi, "Characteristics of the motor programs underlying arm movements in monkeys," J. Neurophysiol., vol. 42, pp. 183–194, 1979.
[2] N. Hogan, "An organizing principle for a class of voluntary movements," J. Neurosci., vol. 4, no. 11, pp. 2745–2754, 1984.
[3] S. Arimoto, S. Kawamura and F. Miyazaki, "Bettering operation of robots by learning," J. Robot. Syst.,vol. 1, no. 2, pp. 123–140, 1984.
[4] Y. Wang, F. Gao and F.J. Doyle III, "Survey on iterative learning control, repetitive control, and run-to-run control," J. Process Control, vol. 19, no. 10, pp. 1589–1600, 2009.
[5] K. Tahara, S. Arimoto, M. Sekimoto and Z.W. Luo, "On control of reaching movements for musculo-skeletal redundant arm model," Applied Bionics and Biomechanics, vol. 6, no. 1, pp. 57–72, 2009.
[6] K. Tahara and H. Kino, "Reaching movements of a redundant musculoskeletal arm: Acquisition of an adequate internal force by iterative learning and its evaluation through a dynamic damping ellipsoid," Adv. Robot., vol. 24, no. 5–6, pp. 783–818, 2010.
[7] M. L. Audu and D. T. Davy, "The inuence of muscle model complexity in musculoskeletal motion modeling," J. Biomech. Eng., pp. 147–157, 1985.
[8] S. Kawamura, F. Miyazaki and S. Arimoto, "Realization of robot motion based on a learning method," IEEE Trans. Sys., Man, Cybern., vol. 18, no. 1, pp. 126–134, 1988.
[9] S. Arimoto, "Robustness of learning control for robot manipulators," IEEE Int. Conf. Robot. Automat., pp. 1528–1833, 1990.
[10] T. Flash and N. Hogan, "The coordination of arm movements: An experimentally confirmed mathematical model," J. Neurosci., vol. 5, no. 7, pp. 1688–1703, 1985.
[11] R. VanRullen and C. Koch, "Visual selective behavior can be triggered by a feed-forward process," J. Cog. Neurosci., vol. 15, no. 2, pp. 209–217, 2003
[12] E. Kosmidis, "Feed-forward inhibition in the visual thalamus," Neurocomp., vol. 44–46, pp. 479–487, 2002.
[13] U. Windhorst, "Muscle proprioceptive feedback and spinal networks," Brain Res. Bulletin, vol. 73, 155-202, 2007.